THE ASTRONOMICAL JOURNAL, 122:3305–3312, 2001 December

INFRARED SPACE OBSERVATORY SHORT WAVELENGTH SPECTROMETER OBSERVATIONS OF V1425 AQUILAE (NOVA AQUILA 1995)

J. E. LYKE,[1] R. D. GEHRZ,[1] C. E. WOODWARD,[1] M. J. BARLOW,[2] D. PÉQUIGNOT,[3] A. SALAMA,[4] G. J. SCHWARZ,[5] S. N. SHORE,[6] S. STARRFIELD,[7] A. EVANS,[8] R. GONZALES-RIESTRA,[9] M. A. GREENHOUSE,[10] R. M. HJELLMING,[11] R. M. HUMPHREYS,[1] T. J. JONES,[1] J. KRAUTTER,[12] C. MORISSET[13] H. B. ÖGELMAN,[14] M. ORIO,[14,15] R. M. WAGNER,[16] N. A. WALTON,[17] AND R. E. WILLIAMS[18]

Received 2000 December 13; accepted 2001 August 20

ABSTRACT

We present observations of the classical nova V1425 Aquilae (Nova Aquila 1995) with the *Infrared Space Observatory*'s (*ISO*) Short Wavelength Spectrometer, the Isaac Newton Telescope's Intermediate Dispersion Spectrograph, and the *International Ultraviolet Explorer*'s Short-Wavelength Primary Spectrograph. Analysis of He II (1640 Å) development constrains the white dwarf turnoff to ~400 days after outburst. Photoionization modeling of the optical and *ISO* spectra obtained during the late nebular phase constrains the mass of the ejecta between 2.5–4.2 × 10^{-5} $M_{\odot}$. This modeling also suggests C and O in the ejecta were enhanced by a factor of ~9, and N was enhanced by a factor of ~100 with respect to solar, while Ne was only slightly enhanced. Based upon these analyses, we determine that the white dwarf in the V1425 Aql system has a CO composition and is at a distance of 3.0 ± 0.4 kpc.

Key words: circumstellar matter — novae, cataclysmic variables — stars: individual (Nova Aquila 1995 = V1425 Aquilae)

1. INTRODUCTION

Classical novae are the result of a thermonuclear runaway on the surface of a white dwarf (WD) in a close binary system. Typically between 10^{-6} and 10^{-4} $M_{\odot}$ of CNO-enriched material is ejected at speeds of order 10^3 km s^{-1}. There are two main classes of novae whose outburst characteristics are correlated with the composition of the underlying WD (Gehrz et al. 1998). A nova that originates on a CO WD ("dusty nova") is primarily overabundant in C, N, and O and sometimes forms an optically thick dust shell about 50–100 days after the outburst that is capable of extinguishing the optical output. In contrast, a nova that originates on an ONeMg WD ("neon nova") shows large overabundances of Ne and Mg and typically does not form much dust. Generally, 100–200 days after outburst, all novae can develop strong infrared (IR) forbidden line emission that can provide abundances of elements in the ejecta with respect to hydrogen and helium. These forbidden line transitions also provide a strong cooling source for the low-density astrophysical plasmas typically ejected during the explosion (Osterbrock 1989).

Mason et al. (1996, hereafter Ma96) estimated the outburst date (day 0) of V1425 Aquilae to be JD 2,449, 742.5 ± 4.0 (1995 January 21–29 UT) based on the similarity of its light curve to that of V1668 Cyg. From ground-based photometry, Ma96 discovered the presence of an optically thin dust shell, and their ground-based spectra, obtained between days ~120 and ~140 after outburst, showed strong recombination lines of H I, He I, and He II and forbidden IR emission lines including [Ca VIII], [Si VII], and [Mg VII]. They suggested that V1425 Aql bridges the gap between dusty CO novae and neon novae. Because of the known presence of forbidden IR emission, V1425 Aql was an ideal candidate for additional study. We present here abundance estimates in the ejecta of V1425 Aql obtained by analyzing several epochs of spectroscopic observations with the European Space Agency's *Infrared Space Observatory* Short Wavelength Spectrometer (*ISO* SWS), the Isaac Newton Telescope (INT) using the facility Intermediate Dispersion Spectrograph (IDS), and NASA's *International Ultraviolet Explorer* (*IUE*) archival data.

2. OBSERVATIONS

V1425 Aql was observed five times between 1996 September 16.3 (day 600.3) and 1997 April 25.1 (day 821.1), including two observations on day 775, with *ISO* SWS. The observations used Astronomical Observing Template

[1] Department of Astronomy, School of Physics and Astronomy, University of Minnesota, 116 Church Street, SE, Minneapolis, MN 55455.
[2] Department of Physics and Astronomy, University College London, Gower Street, London WC1E 6BT, UK.
[3] Observatoire de Paris-Meudon, 5 Place Jules Janseen, F-92195 Meudon Cedex, France.
[4] *ISO* Science Operations Centre, Astrophysics Division of ESA, Postbox 50727, E-28080 Villafranca/Madrid, Spain.
[5] Steward Observatory, University of Arizona, 933 North Cherry Avenue, Tucson, AZ 85721.
[6] Department of Physics and Astronomy, Indiana University South Bend, 1700 Mishawaka Avenue, South Bend, IN 46634-7111.
[7] Department of Physics and Astronomy, Arizona State University, P.O. Box 871504, Tempe, AZ 85287.
[8] Department of Physics, Keele University, Keele, Staffordshire ST5 5BG, UK.
[9] ESA, Villafranca del Castillo, Apartado de Correos 50727, E-28080 Madrid, Spain.
[10] NASA Goddard Space Flight Center, Code 685, Greenbelt, MD 20771.
[11] Deceased.
[12] Landessternwarte, Königstuhl, D-69117 Heidelberg, Germany.
[13] Institut d'Astrophysique de Marseille, Traverse du Siphon, BP 8, F-13376 Marseille Cedex 12, France.
[14] Department of Astronomy, University of Wisconsin, Madison, 475 North Charter Street, Madison, WI 53706.
[15] Osservatorio Astronomico di Torino, Strada Osservatorio 20, I-10025 Pino Torinese, Italy.
[16] Large Binocular Telescope Observatory, University of Arizona, 933 North Cherry Avenue, Tucson, AZ 85721.
[17] Isaac Newton Group, Apartado 321, 38700 Santa Cruz de La Palma, Canary Islands, Spain.
[18] Space Telescope Science Institute, 3700 San Martin Drive, Baltimore, MD 21218.

(AOT) SWS01: fast, full-range scans at a resolution of $\lambda/\Delta\lambda \simeq 2000$ (Valentijn et al. 1996), which are detailed in Table 1. This AOT scanned the wavelength range twice (up/down scans), and the data were flagged accordingly. The *ISO* SWS instrument is described in detail in de Graauw et al. (1996). Contemporaneous optical observations of the nova were obtained on 1997 April 27 using the IDS on the 2.5 m INT on La Palma (Laing & Jones 1985). These observations are also detailed in Table 1. To investigate the early evolution of V1425 Aql, we use the Short Wavelength Primary (SWP) spectrograph on board the *IUE*. The SWP has a wavelength coverage of 1150–1980 Å and a resolution of $\lambda/\Delta\lambda \simeq 300$ in low-resolution mode. The *IUE* observation log is listed in Table 2.

3. DATA REDUCTION

3.1. *ISO*

The *ISO* data were reduced using version 10.0 of the *ISO* SWS pipeline and analyzed from the Auto Analysis Result (AAR) level in the Observer's SWS Interactive Analysis and in the *ISO* Spectral Analysis Package (ISAP) version 1.4 (Sturm 1997). The full range of each spectrum is 2.38–45.2 μm and is divided into four bands of 12 detectors each. Bad data were removed by an ISAP task. AOT SWS01 scans the grating twice to produce two data sets for each of the 48 detectors. This allowed us to distinguish real features (that appear in both the up and down scans) from transient noise events, such as cosmic rays. The redundancy of detectors also allowed us to ignore the data from specific detectors, since some detectors were much noisier than others. Within each band, typically three of the 12 detectors were turned off and the remaining data were averaged. Single-component Gaussians were fitted to the averaged lines from which fluxes, line centers, and FWHM velocities were obtained.

3.2. *INT*

The optical data were reduced using the Image Reduction and Analysis Facility (IRAF) version 2.11.3 following the IRAF user's guides by Massey (1997)[19] and Massey, Valdes, & Barnes (1992).[20] To determine the line centers, integrated fluxes, and equivalent widths of the emission lines, the INT nova spectra were fitted with single-component or deblended Gaussians. The fluxes from successive integrations were then averaged according to their integration times. We corrected these averaged fluxes for interstellar reddening using $E(B-V) = 0.76$ from Kamath et al. (1997, hereafter K97) and the interstellar extinction law presented in Rieke & Lebofsky (1985). The relative fluxes derived from the optical spectra match those of the day 843.8 spectrum from K97 within 5%; however, the absolute fluxes do not match because their sky conditions were nonphotometric.

3.3. *IUE*

The ultraviolet spectra were reduced at the Goddard Space Flight Center's Regional Data Analysis Facility using the *NEWSIPS IUE* software and special purpose IDL routines. The integrated line fluxes were dereddened assuming

[19] Available at http://iraf.noao.edu/docs/recommend.html.
[20] Available at http://iraf.noao.edu/docs/recommend.html.

TABLE 1

ISO/INT Observational Details

Description	Wavelength Range[a]	Date	Time (UT)	Exposure (s)	Days Since Outburst (± 4)[b]
ISO SWS01[c].....	2.38–45.2	1996 Sep 16	0639	3450	600.3
ISO SWS01	2.38–45.2	1996 Oct 31	1715	3450	645.7
ISO SWS01	2.38–45.2	1997 Mar 10	0630	3450	775.3
ISO SWS01	2.38–45.2	1997 Mar 10	2139	3450	775.9
ISO SWS01	2.38–45.2	1997 Apr 25	0300	3450	821.1
INT IDS.....	3400–6750	1997 Apr 27	0420	240	823.1
INT IDS.....	3400–6750	1997 Apr 27	0431	600	823.1
INT IDS.....	3400–6750	1997 Apr 27	0442	600	823.1
INT IDS.....	6600–10000	1997 Apr 27	0503	600	823.1
INT IDS.....	6600–10000	1997 Apr 27	0519	1200	823.1

[a] Wavelength units are microns for *ISO* SWS and angstroms for INT IDS.
[b] Day 0 is determined by Mason et al. 1996.
[c] SWS AOTs are described in de Graauw et al. 1996.

TABLE 2

IUE Observation Log

Image Number	Date	Time (UT)	Exposure (s)	He II (1640 Å) Flux[a]	Days Since Outburst (± 4)[b]
SWP 54119.....	1995 Mar 3	1559	420	3.05 ± 0.25	37.7
SWP 54160.....	1995 Mar 17	0232	600	3.10 ± 0.30	51.1
SWP 54243.....	1995 Mar 28	0134	600	2.25 ± 0.25	62.1
SWP 54244.....	1995 Mar 28	0224	1500	2.45 ± 0.25	62.1
SWP 54439.....	1995 Apr 15	2312	900	1.40 ± 0.10	80.9
SWP 54440.....	1995 Apr 16	0007	1800	1.45 ± 0.15	81.0

[a] The flux values are times 10^{-12} ergs cm^{-2} s^{-1}.
[b] Day 0 is determined by Mason et al. 1996.

an $E(B-V) = 0.76$ (K97) and the extinction law of Seaton (1979).

4. RESULTS AND DISCUSSION

4.1. *Emission Lines*

Sample *ISO* spectra are presented in Figures 1 and 2, and the measured *ISO* emission-line fluxes are summarized in Table 3. Because of the faintness of the source, the only persistent lines in our spectra are [Ne VI] 7.65 μm, [O IV] 25.89 μm, and [Ne V] lines at 14.3 and 24.3 μm. We find significant changes in the fluxes of emission lines for the spectra obtained on day 775. We attribute these changes to variations in the instrumental sensitivity rather than physical changes in the ejecta, and therefore we average our day 775 fluxes in our empirical analysis.

The [O IV] line has a constant intensity over the course of our observations, the [Ne V] 14.3 μm line remains constant from day 645 to day 775, but the [Ne VI] 7.65 μm line declines in intensity over the same period. The FWHM velocities of the [Ne VI] 7.65 μm and [O IV] 25.89 μm lines

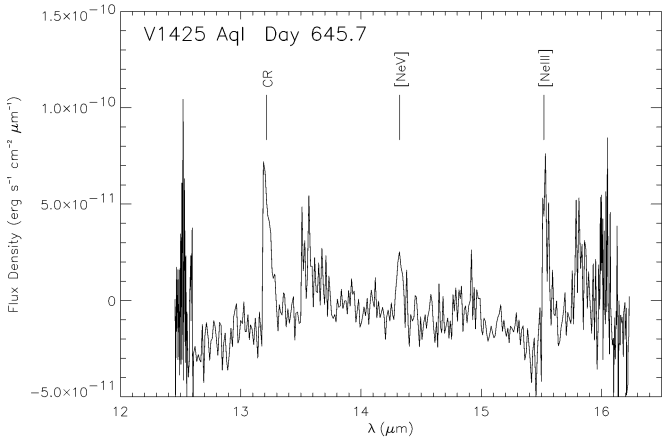

FIG. 1.—Averaged *ISO* SWS spectrum from day 645.7. Data from detectors 28, 31, 34, and 36 have been ignored, bad data points have been removed, and the remaining detectors have been averaged. The features are a cosmic-ray hit (CR), [Ne V] 14.3 μm, and [Ne III] 15.5 μm.

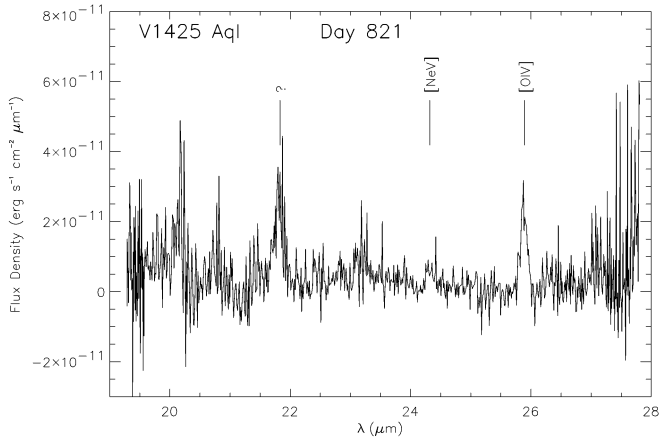

FIG. 2.—Same as Fig. 1, but from day 821.1. The lines are [Ne V] 24.3 μm, [O IV] 25.9 μm, and an unidentified line at 21.8 μm that is probably not [Ar III] despite the wavelength coincidence.

are different ($\sim$800 and $\sim$1500 km s^{-1}, respectively), indicating that these lines arise at different ejecta radii. The excitation potentials of the ions observed indicates that the ionizing flux contains photons with energies up to $\geq$126.2 eV [Ne VI]. Dense clumps in the ejecta that shield regions from hard, ionizing flux is one possible explanation for this extreme range of ions ([O I], [Ne VI]; Williams 1992; and see also § 4.4).

We did not detect [Ne II] 12.8 μm emission in our *ISO* spectra. However, we observed strong emission from [Ne VI] 7.65 μm. We attribute this to the expansion of the ejecta while the effective temperature of the WD increased, driving ionization to higher states (Gehrz et al. 1998). The observations of the neon nova V1974 Cyg show that the decline of [Ne II] emission is correlated with the rise of [Ne VI] emission (Hayward et al. 1996) but that [Ne II] emission recovers past day 800. Using the average ratio of [Ne II]/[Ne VI] = 0.036 from days 849 and 882 in V1974 Cyg, we estimate an upper limit to [Ne II] 12.8 μm = 4.3×10^{-14} ergs cm^{-2} s^{-1}.

We present the INT optical spectrum (day 823.1) in Figure 3. These lines are presented in Table 4 along with the

TABLE 3

ISO EMISSION LINES

λ[c] (μm)	Identity	Day 600.3	Day 645.7	Day 775.3	Day 775.9	Day 821.1
7.652:						
Flux[a]	[Ne VI]	1.8 ± 0.2	1.6 ± 0.3	0.8 ± 0.2	1.0 ± 0.6	1.2 ± 0.2
FWHM Velocity[b]		760 ± 30	900 fixed	790 ± 50	900 fixed	760 ± 25
14.322:						
Flux[a]	[Ne V]	...	2.4 ± 0.7	1.4 ± 0.7	3.0 ± 0.9	≤1.3
FWHM Velocity[b]			1660 ± 60	1350 ± 100	1450 ± 70	...
24.318:						
Flux[a]	[Ne V]	...	...	...	...	0.6 ± 0.3
FWHM Velocity[b]						1600 fixed
25.890:						
Flux[a]	[O IV]	4.5 ± 0.5	4.3 ± 0.5	4.6 ± 0.7	5.1 ± 0.5	3.7 ± 0.5
FWHM Velocity[b]		1500 ± 30	1430 ± 30	1400 ± 30	1700 ± 20	1410 ± 20

[a] The flux values are times 10^{-12} ergs cm^{-2} s^{-1}.
[b] The velocity units are km s^{-1}.
[c] Wavelengths are taken from Feuchtgruber et al. 1997.

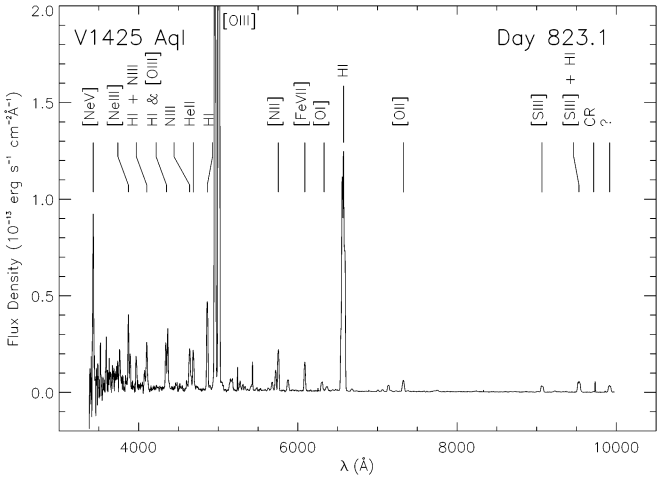

FIG. 3.—Dereddened INT IDS spectrum (600 s) showing several prominent emission lines, including [Ne v] 3426 Å, [Ne iii] 3870 Å, the [O iii] doublet near 5000 Å, [O ii] 7320 + 7330 Å, and the Balmer series.

TABLE 4

EMISSION LINES NEAR DAY 820

λ (μm)	Identity	Dereddened Flux[a]	FWHM (km s^{-1})
0.3426.....	[Ne v]	1.492	1590
0.3870.....	[Ne iii]	0.695	880
0.3889.....	H i	0.302	1070
0.3970.....	H i + [Ne iii]	0.385	...
0.4074.....	[S ii] blend	0.173	...
0.4101.....	Hδ + N iii	0.470	...
0.4340.....	Hγ	0.412	980
0.4363.....	[O iii]	0.447	870
0.4640.....	N iii + blend	0.438	...
0.4686.....	He ii	0.352	1100
0.4861.....	Hβ	1.000	1080
0.4896.....	[Fe iii]	0.104	1270
0.4959.....	[O iii]	8.713	1100
0.5007.....	[O iii]	23.879	1070
0.5176.....	[Fe vi]	0.146	850
0.5677.....	[Fe vi]	0.101	550
0.5721.....	[Fe vii]	0.208	...
0.5755.....	[N ii]	0.465	910
0.5876.....	He i	0.149	1100
0.6087.....	[Fe vii] + [Ca v]	0.329	...
0.6300.....	[O i]	0.156	1220
0.6363.....	[O i]	0.058	1360
0.6563.....	Hα + [N ii]	5.656	...
0.6678.....	He i	0.033	1170
0.7005.....	[Ar v]	0.020	880
0.7065.....	He i	0.028	1090
0.7136.....	[Ar iii]	0.104	1100
0.7237.....	?	0.013	1270
0.7325.....	[O ii] blend	0.181	...
0.7378.....	[Ni ii] ?	0.014	1210
0.7876.....	[P ii] ?	0.009	1390
0.8237.....	He ii	0.023	1960
0.9015.....	H i	0.010	1120
0.9066.....	[S iii]	0.132	1110
0.9229.....	H i	0.020	1050
0.9531.....	[S iii] + H i	0.252	...
0.9918.....	?	0.131	1000
7.652	[Ne vi]	1.30	760
24.318.....	[Ne v]	0.65	1600
25.890.....	[O iv]	4.0	1420

[a] Relative to $F_{H\beta} = 9.254 \times 10^{-13}$ ergs cm^{-2} s^{-1}.

ISO day 821.1 lines. At this stage, the nova shows nebular lines of [O iii] (4363, 4959, 5007 Å), [Ne v] (3426 Å), [N ii] (5755 Å), and [O ii] (7320 + 7330 Å), as well as hydrogen recombination lines and Fe lines. We use the [O iii] and [Ne v] lines, including the [Ne v] 24.3 μm line from the *ISO* spectrum of day 821.1, to determine the electron temperature (T_e) and electron density (n_e) of the ejecta. For T_e, we use average collision strengths as described in Osterbrock (1989):

$$\frac{j_{\lambda 4959} + j_{\lambda 5007}}{j_{\lambda 4363}} = \frac{7.73 \exp\left[(3.29 \times 10^4)/T_e\right]}{1 + 4.5 \times 10^{-4}(n_e/T_e^{1/2})} . \quad (1)$$

We could not estimate n_e from the standard [O ii] line ratio since it could not be determined because of blending from the large ejection velocities. Thus we used line ratios from other ions and the IRAF task NEBULAR.IONIC (Shaw & Dufour 1995), which solves the equations of thermal and statistical equilibrium assuming a five-level atom and yields solutions for T_e and n_e. The [Ne v] line ratio $I_{\lambda 24.3}/I_{\lambda 0.3426}$ provides a complementary equation to equation (1) to determine n_e. Using [Ne v] collision strengths from Lennon & Burke (1991) and transition probabilities from Nussbaumer & Rusca (1979) and our ratios [O iii] ($(I_{\lambda 4959} + I_{\lambda 5007})/I_{\lambda 4363} = 72.9$) and [Ne v] ($I_{\lambda 24.3}/I_{\lambda 0.3426} = 0.40$), we determine $n_e = 3.5 \times 10^4$ cm^{-3} and $T_e = 13{,}800$ K. In addition, we used the [N ii] flux for another estimate of n_e. We measured $I(\mathrm{H}\alpha + [\mathrm{N\ II}])/I(\mathrm{H}\beta) = 5.656$. Since the theoretical case B Hα/Hβ ratio is ~2.8, the observed Hα + [N ii] blended line implies $n_e = 2.1$–4.6×10^5 cm^{-3} ($T_e = 15{,}000$–$10{,}000$ K). This factor of 10 in the n_e determinations demonstrates the "clumpiness" of the ejecta, since shielded low-ionization species would be expected in denser regions of the ejecta.

Using $T_e = 13{,}800$ K and $n_e = 3.5 \times 10^4$ cm^{-3} and the Balmer line ratios and emissivities from Storey & Hummer (1995), we find that Brackett α and Humphreys α would not be observable with *ISO* SWS.

4.2. *WD Turnoff*

To indirectly probe the photoionization conditions of the ejecta and to constrain the end of nuclear burning on the WD surface, we use a method developed by Shore, Starrfield, & Sonneborn (1996). Nova ejecta preserve their ionization state even after the cessation of X-ray illumination by the central star because of ejecta expansion. This is particularly simple because of the power-law density distribution and linear velocity law found for the ejecta. In V1974 Cyg, the evolution of the He ii 1640 Å line was fitted by a recombination model in an expanding shell after the observed X-ray turnoff. This technique has since been used to obtain turnoff times for a large number of novae (Schwarz et al. 2001; Vanlandingham et al. 2001), and we apply it here to V1425 Aql.

In the constant mass ejecta, the expansion remains self-similar and the density declines as t^{-3}, so the He ii emission measure from recombinations varies as

$$\ln(j_{1640}/j_0) = \tfrac{1}{2}\alpha n_{e,0}\, t_0[(t_0/t)^2 - 1] . \quad (2)$$

Here j_{1640} is the He ii emission measure, j_0 is the He ii emission measure at turnoff, t_0 is the turnoff time, α is the He ii (1640 Å) recombination coefficient (2.2×10^{-12} cm^3 s^{-1}; Osterbrock 1989), and $n_{e,0}$ is the electron density at turnoff.

In Figure 4, we show the development of He II (1640 Å) emission for V1425 Aql. We convert the observed He II (4686 Å) from INT spectrum to He II (1640 Å) using the theoretical He II 1640/4686 ratio of ≈ 7 (Osterbrock 1989). With no a priori knowledge of the distance to V1425 Aql, we plot each observation as a solid vertical line with crosses providing the distance used to calculate the He II luminosity. The distances are labeled to the right of the INT luminosities.

We used the CLOUDY 90.03 photoionization code developed by Ferland (1996 and references therein) and collaborators to obtain the He II (1640 Å) luminosity for recombination models with various turnoff times. Assuming a blackbody illuminating source, each CLOUDY model used the following input parameters: an effective temperature of 3×10^5 K, a luminosity of 10^{38} ergs s^{-1}, a filling factor of 0.1 (consistent with the degree of clumpiness observed in the *IUE* long-wavelength primary high-resolution spectra obtained at the same time as the first two *IUE* SWP spectra), a density law proportional to r^{-3}, and solar abundances. The nova shell dimensions were defined by the observed range in the early expansion velocities (1000–2000 km s^{-1}) and a Hubble flow, $v = rt$. The model electron density at turnoff, $n_{e,0}$, was calculated by interpolating the derived density backward from day 820 to day 0, assuming a t^{-3} dependence. This model corresponds to a freely expanding shell in which the shell changes thickness at a constant rate while the shell expands at a constant velocity. The electron density on day 820 was fixed at $\sim 10^5$ cm^{-3}, which is consistent with the values determined from the line ratios (§ 4.1). The ejected mass determined by the CLOUDY model is $2.5 \times 10^{-5}\ M_\odot$ in good agreement with the mass range determined by K97. In Table 5 we present the electron densities and CLOUDY determined He II (1640 Å) luminosities for different turnoff times. The data from Table 5 were used in equation (2) to produce the dotted lines in Figure 4. The beginning of each He II (1640 Å) recombination model is labeled by its respective turnoff date. Note that the evolution of each model is highly dependent on the electron density at turnoff.

Given the uncertainties and assumptions, there is remarkable agreement between the observations and the models. An independent estimate of the distance can be calculated using a maximum magnitude versus rate of decline relationship (MMRD) and assuming that the optical light curve of V1425 Aql was exactly like V1668 Cyg (Ma96). Using the MMRD relation given in Della Valle & Livio (1998), a $t_2 = 11$ days, $m_V = 5.9$–6.5, and $E(B-V) = 0.76$ provides a distance of 3000 ± 400 pc. The most consistent fit to the observations and distance is a turnoff date of 400 ± 100 days. The quick turnoff is in good agreement with the rapid turnoff times determined for other fast novae (Vanlandingham et al. 2001).

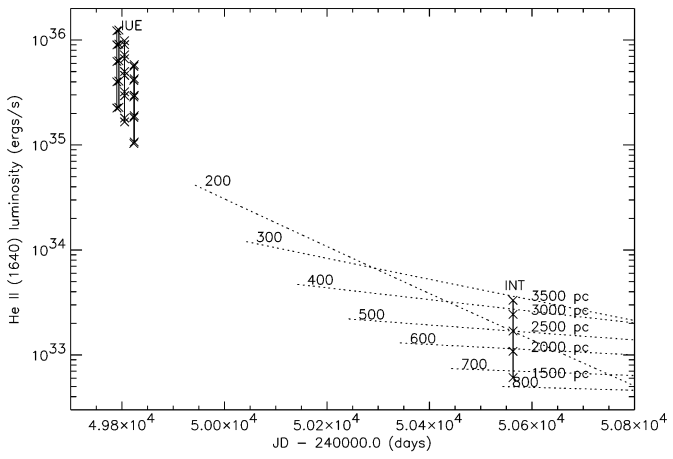

FIG. 4.—He II (1640 Å) emission development using *IUE* observations and INT He II (4686 Å) flux converted to He II (1640 Å) using the theoretical He II 1640/4686 ratio given by Osterbrock (1989). To the right of the INT values are the distances (in parsecs) used to convert fluxes to luminosities. We determine WD turnoff to be 400 ± 100 days.

TABLE 5

WD TURNOFF MODEL PARAMETERS

Turnoff Date (days since outburst)	$n_{e,0}$ (cm^{-3})	He II (1640 Å) Luminosity (ergs s^{-1})
100	5.5×10^7	4.4×10^{35}
200	6.9×10^6	4.1×10^{34}
300	2.0×10^6	1.2×10^{34}
400	8.6×10^5	4.7×10^{33}
500	4.4×10^5	2.2×10^{33}
600	2.6×10^5	1.3×10^{33}
700	1.6×10^5	7.4×10^{32}
800	1.1×10^5	5.0×10^{32}

Radiation pressure–driven wind models (Starrfield et al. 1991; Vanlandingham et al. 2001) show that the turnoff time is a function of the WD mass. Thus the ~ 1 yr turnoff time estimated for V1425 Aql implies that its underlying WD is massive. This conclusion is consistent with the rapid light curve decline and the large expansion velocities observed.

4.3. *Empirical Nebular Analysis*

With the simplistic assumption of uniform ejecta, we can estimate the ionic abundances of the various elements observed in the ~ 820 optical and *ISO* spectra. Using our measurement for Hβ on day 823, we determined ionic abundances with respect to H^+ using volume emissivities calculated by the NEBULAR.IONIC task (Shaw & Dufour 1995):

$$\frac{n(X^{+p})}{n(\mathrm{H})} = \frac{I(\lambda)}{I(\mathrm{H}\beta)} \frac{j(\mathrm{H}\beta)}{j(\lambda)}, \tag{3}$$

where $I(\lambda)/I(\mathrm{H}\beta)$ is the observed line ratio and the j's are the calculated volume emissivities. This method assumes that the two emission lines arise in regions with the same T_e and n_e, which clearly does not hold, yet provides a first-order abundance estimate of the ejecta. We present these abundances in Table 6. Summing the abundances of different ions gives a lower limit to the elemental abundances. An interpolation between Ne^{2+} and Ne^{4+} provides an estimate of $n(Ne^{3+})/n(H^+) = 3.37 \times 10^{-5}$. A similar interpolation between Ar^{2+} and Ar^{4+} provides an estimate of $n(Ar^{3+})/n(H^+) = 3.28 \times 10^{-7}$. The N^+/O^+ ratio, based upon lines with roughly similar dependence on T_e and n_e, is much larger than the solar N/O, suggesting that N is highly overabundant in the ejecta.

4.4. *Modeling Analysis*

Recognizing the need for a more rigorous abundance determination, we also used the photoionization code

TABLE 6

EMPIRICAL ABUNDANCES NEAR DAY 820

Ion	Line λ (μm)	I(line)/I(Hβ)	n(Ion)/n(H$^+$)	By Number vs. Solar[a]
N^{+1}.....	0.5755	0.465	9.59×10^{-5}	0.85
O^0.....	0.6300	0.156	1.03×10^{-5}	...
O^0.....	0.6363	0.058	1.19×10^{-5}	...
O^{+1}.....	0.7320 + 0.7330	0.180	1.57×10^{-5}	...
O^{+2}.....	0.4959 + 0.5007	32.59	3.33×10^{-4}	...
O^{+2}.....	0.4363	0.447	3.34×10^{-4}	...
O^{+3}.....	25.890	3.40	4.71×10^{-4}	0.98
Ne^{+2}.....	0.3868	0.695	2.43×10^{-5}	...
Ne^{+4}.....	0.3426	1.49	4.27×10^{-5}	...
Ne^{+4}.....	24.318	0.648	4.33×10^{-5}	...
Ne^{+5}.....	7.6524	1.30	1.29×10^{-5}	0.96[b]
Ar^{+2}	0.7136	0.104	4.86×10^{-7}	...
Ar^{+4}	0.7005	0.020	1.71×10^{-7}	0.27[c]
Fe^{+5}	0.5177	0.146	1.80×10^{-5}	...
Fe^{+5}	0.5674	0.101	1.35×10^{-5}	...
Fe^{+6}	0.6087	0.329	1.06×10^{-5}	...
Fe^{+6}	0.5722	0.208	1.01×10^{-5}	0.75

[a] Solar abundances from Cox 2000.
[b] Includes interpolated $n(Ne^{3+})/n(H^+)$.
[c] Includes interpolated $n(Ar^{3+})/n(H^+)$.

NEBU (see Petitjean, Boisson, & Péquignot 1990; Morisset & Péquignot 1996; Péquignot et al. 2001) to determine abundances and other nova properties on day 822. This code solves the equations for thermal equilibrium, statistical equilibrium, and radiation transfer in spherical symmetry. The model shell, based on a consistent combination of spherical computations, is made up of a relatively transparent low-density medium of large covering factor in which higher density radiation-bounded clumps, with small overall covering factor, are embedded and therefore partly shielded from the primary radiation. This two-component shell involves six parameters (the filling factor is always unity). The outer radius of the shell is taken as 8×10^{15}cm (expansion velocity 1125 km s^{-1} from optical line profiles). The central source spectrum is a blackbody (temperature T_{BB} and luminosity L_{BB}), with a discontinuity at the He$^+$ ionization limit (flux multiplied by a constant arbitrary factor $f_{4\ ryd}$ above 4 ryd). The He, N, O, Ne, S, Ar, and Fe abundances are strongly constrained by observation, while C is very poorly constrained. The 17 or so model parameters are adjusted until model spectra satisfactorily reproduce the observed spectra. Since a good fit could be obtained and the observational constraints (including recombination lines, not explicitly considered here) largely outnumber the free parameters of the model, the results are significant. Given that the solution is neither perfect nor strictly unique and considering the observational and theoretical uncertainties, the derived abundances are uncertain by perhaps 50% (20% for helium), although abundance ratios are more accurately determined. More details will be given elsewhere (Péquignot 2001). Some basic properties of a particularly successful model are provided in Tables 7 (central source), 8 (shell), and 9 (elemental abundances).

Since $f_{4\ ryd}$ is much less than unity and T_{BB} is large, the luminosity L_{eff} and effective temperature T_{eff} (Table 7) are less than the blackbody values. The value of L_{eff} is a few percent of the Eddington limit, confirming that the turnoff occurred well before day 822 and that cooling to the WD stage was very fast. The large discontinuity implied by the model is in qualitative agreement with expectations, considering that (1) T_{eff} is not extremely high, (2) the gravitational field is very large ($\log g \sim 7.5$), and (3) soon after hydrogen exhaustion, the atmosphere of the WD must be composed mainly of helium.

The photoionization model approach will be self-consistent if departures from ionization and thermal

TABLE 7

MODEL STAR PROPERTIES ON DAY 822

Property	Value
T_{BB} (K)	2.2×10^5
L_{BB} (ergs s^{-1}).....	8.0×10^{36}
$f_{4\ ryd}$.....	0.12
T_{eff} (K)	1.8×10^5
L_{eff} (ergs s^{-1}).....	3.5×10^{36}
R_* (cm).....	2.2×10^9
$\log g$	~ 7.5

TABLE 8

MODEL SHELL PROPERTIES ON DAY 822

Quantity	Diffuse	Clumps
$\langle n_H \rangle$ (cm^3)	4.5×10^4	2.2×10^5
Filling factor.....	1.0	1.0
$\langle T \rangle$ (K)	13000	7000
Thickness (cm).....	1.1×10^{15}	1.7×10^{14}
Covering factor[a]	0.63	0.021
Mass ($M_\odot$)	3.6×10^{-5}	0.64×10^{-5} [b]
fraction I_{beta} (%).....	25	75
$\tau_{13.6}$.....	0.085	(130)[c]
$\tau_{54.4}$.....	0.43	(60)[c]

[a] For a distance of 2.7 kpc.
[b] Minimum mass.
[c] Radiation bounded ($T_{end} = 3000$ K).

TABLE 9

MODEL ABUNDANCES ON DAY 822

Element (1)	By Number (2)	By Mass (3)	By Mass vs. Solar[a] (4)
H	1.000	0.504	0.71
He.....	0.132	0.266	0.96
C	5×10^{-3}	0.030	9.0
N	15.0×10^{-3}	0.106	96.0
O	10.5×10^{-3}	0.085	8.8
Ne.....	46.0×10^{-5}	0.0046	2.7
S.....	2.0×10^{-5}	0.0003	0.8
Ar	0.51×10^{-5}	0.00010	1.0
Fe	5.2×10^{-5}	0.0015	1.1

[a] Solar abundances from Cox 2000.

balance are moderate. The recombination coefficients for many ions 3+, 4+ observed in the shell are $\alpha = (2.0–6.0) \times 10^{-11}$ cm^3 s^{-1}, leading to a typical recombination timescale in the highly ionized medium $t_{\rm rec} = (10–3)$ days$/(n_e/6 \times 10^4$ cm$^{-3})$, that is 1 week or less. In the clumps, n_e is 4–5 times larger and the α's are 1 order of magnitude less (they are somewhat enhanced because of the lower T), although α is even smaller for hydrogen. However, the gas cooling timescale, $t_{\rm cool}$, of the order of 1 month in the diffuse medium, is much less than 1 week in the bulk of the clumps. Hence, if approximate equilibrium were not achieved, the temperature would decline drastically, leading to faster recombination and contributing to restoring ionization equilibrium. In summary, the typical timescale for equilibration should be as short as 1 week everywhere in the shell. This is probably shorter than the WD shrinking time scale. We remind the reader that the spectral differences between days 821 and 844 are negligible.

Assuming a distance of 2.7 kpc, the total covering factor of the shell is about 0.63 (Table 8). The covering factor is the only quantity in the model that depends on the distance. Since this factor cannot exceed unity, the maximum distance allowed is 3.3 kpc, in agreement with other estimates (§ 4.2). The total mass ejected is $4.2 \times 10^{-5}\ M_\odot$ in good agreement with the determination in (§ 4.2) and in K97 ($\sim 10^{-4}\ M_\odot$).

In column (2) of Table 9, abundances are given by number relative to H. However the abundances by mass (col. [3]) are much more significant for this H-deficient material. In column (4), these abundances by mass are compared with those of the solar system. Argon, and iron, which are not synthesized in either the parent star or the nova outburst, have nearly solar abundances, pointing to a Population I origin of the binary. Within uncertainties, sulfur was not synthesized either, in agreement with the CO nova interpretation.

Nitrogen and oxygen are strongly enhanced (Table 9), as expected in CO nova shells. Note that the abundances from our modeling are much larger than found in the empirical estimates (Table 6), mainly as a consequence of the strong temperature gradient across the shell. Specifically, a dominant fraction of Hβ arises from the relatively cool clumps (Table 8), whereas [O III] 4363 Å, extremely sensitive to T_e, is partly produced in the highly ionized gas, in which O^{2+} is not the dominant ion of oxygen. Then, the uniform temperature adopted in the empirical approach is biased toward too high a value. The two abundance estimates for iron are not too different just because, in this case, the dominant (observed) ions mainly belong to the hot component of the shell.

Neon, well diagnosed by several lines from several ions, is significantly overabundant (Table 9) but to a lesser extent than nitrogen and oxygen. The neon overabundance is not sufficient to imply that the WD was of the ONeMg type (Livio & Truran 1994). Because of the high overabundance of CNO (especially N), the abundances are most consistent with a CO WD interpretation.

A rather definite picture of the nova shell can be obtained assuming stationary photoionization, despite the fast cooling of the post nova. The far-IR lines observed by *ISO*, particularly [O IV], played a vital role in narrowing the range of acceptable models and in establishing with some certainty the set of elemental abundances.

5. CONCLUSIONS

Early *IUE* and late optical spectra showed that nuclear burning on the WD of the V1425 Aql system had turned off $\sim$400 days after outburst, prior to our *ISO* SWS observations. We observed persistent cooling lines of [Ne VI] 7.65 μm and [O IV] 25.89 μm more than 400 days after the WD turnoff with *ISO* SWS. The [O IV] 25.89 μm line is one of the most prominent emission lines in all novae we observed with *ISO* SWS (Lyke et al. 2001). Expansion rates inferred from the FWHM velocities of the [Ne VI] and [O IV] lines indicate the ejecta are inhomogeneous. Contemporaneous to our day 821 *ISO* observation, we observed optical nebular lines including [O III] (4363, 4959, 5007 Å), [Ne V] (3426 Å), [N II] (5755 Å), and [O II] (7320 + 7330 Å), as well as hydrogen recombination lines and Fe lines. We determined different n_e values from ratios of [Ne V] lines compared with ratios of [N II] lines further indicating nonuniform ejecta.

We estimate the mass of the ejecta as $2.5–4.2 \times 10^{-5}\ M_\odot$ using our WD turnoff analysis and our two-component ejecta model. This mass estimate agrees with the $\sim 10^{-4}$ $M_\odot$ value from K97. Using three separate methods, we determine the distance to V1425 Aql as 3.0 ± 0.4 kpc.

Using a two-component model for the ejecta, we determine the ejecta of V1425 Aql is enriched in CNO with respect to solar (C and O by a factor of $\sim$9 and N by a factor of $\sim$100) and slightly enriched in heavier elements (Ne by a factor of $\sim$3 and S, Ar, and Fe solar). These abundances are consistent with a CO WD as the progenitor of V1425 Aql.

J. E. L., R. D. G., and C. E. W. were supported by an *ISO* block grant. S. S. would like to acknowledge partial support to Arizona State University from NASA and NSF grants. The *Infrared Space Observatory* (*ISO*) is an ESA project with instruments funded by ESA member states (especially the PI countries: France, Germany, the Netherlands, and the UK) and with the participation of ISAS and NASA. The *ISO* Spectral Analysis Package (ISAP) is a joint development by the LWS and SWS Instrument Teams and Data Centers. Contributing institutes are CESR, IAS, IPAC, MPE, RAL and SRON. The Isaac Newton Telescope is operated on the island of La Palma by the Isaac Newton Group in the Spanish Observatorio del Roque de los Muchachos of the Instituto de Astrofisica de Canarias.

REFERENCES

Cox, A. N., ed. 2000, Allen's Astrophysical Quantities (4th ed.; New York: Springer)
de Graauw, Th., et al. 1996, A&A, 315, L49
Della Valle, M., & Livio, M. 1998, ApJ, 506, 818
Ferland, G. J. 1996, Dept. Phys. & Astron. Internal Report (Lexington: Univ. Kentucky)
Feuchtgruber, H., et al. 1997, ApJ, 487, 962
Gehrz, R. D., Truran, J. W., Williams, R. E., & Starrfield, S. 1998, PASP, 110, 3
Hayward, T. L., et al. 1996, ApJ, 469, 854
Kamath, U. S., Anupama, G. C., Ashok, N. M., & Chandrasekhar, T. 1997, AJ, 114, 2671
Laing, R., & Jones, D. 1985, Vistas Astron., 28, 483
Lennon, D. J., & Burke, V. M. 1991, MNRAS, 251, 628
Livio, M., & Truran, J. W. 1994, ApJ, 425, 797
Lyke, J. E., et al. 2001, in preparation
Mason, C. G., Gehrz, R. D., Woodward, C. E., Smilowitz, J. B., Greenhouse, M. A., Hayward, T. L., & Houck, J. R. 1996, ApJ, 470, 577
Massey, P. 1997, A User's Guide to CCD Reductions with IRAF (Tucson: KPNO Comput. Support Group)
Massey, P., Valdes, F., & Barnes, J. 1992, A User's Guide to Reducing Slit Spectra with IRAF (Tucson: NOAO)
Morisset, C., & Péquignot, D. 1996, A&A, 312, 135
Nussbaumer, H., & Rusca, C. 1979, A&A, 72, 129
Osterbrock, D. E. 1989, Astrophysics of Gaseous Nebulae and Active Galactic Nuclei (Mill Valley: Univ. Sci.)
Péquignot, D. 2001, in preparation
Péquignot, D., et al. 2001, PASP, in press
Petitjean, P., Boisson, C., Péquignot, D. 1990, A&A, 240, 433
Rieke, G. H., & Lebofsky, M. J. 1985, ApJ, 288, 618
Schwarz, G. J., Shore, S. N., Starrfield, S., Hauschildt, P. H., Della Valle, M., & Baron, E. 2001, MNRAS, 320, 103
Seaton, M. J. 1979, MNRAS, 187, 73P
Shaw, R. A., & Dufour, R. J. 1995, PASP, 107, 896
Shore, S. N., Starrfield, S., & Sonneborn, G. 1996, ApJ, 463, L21
Starrfield, S., Truran, J. W., Sparks, W. M., & Krautter, J. 1991, in Extreme Ultraviolet Astronomy, ed. R. F. Malina & S. Bowyer (New York: Pergamon), 168
Storey, P. J., & Hummer, D. G. 1995, MNRAS, 272, 41
Sturm, E. 1997, Ap&SS, 258, 285
Valentijn, E. A., et al. 1996, A&A, 315, L60
Vanlandingham, K. M., Schwarz, G. J., Shore, S. N., & Starrfield, S. 2001, AJ, 121, 1126
Williams, R. E. 1992, ApJ, 392, 99